Study of the effect of finite extent on sound transmission loss of single panel using a waveguide model

Iwan Prasetiyo, David Thompson

ACOUSTICS 2012

Study of the effect of finite extent on sound transmission loss of single panel using a waveguide model

I. Prasetiyo and D. J. Thompson

Dynamics Group - ISVR - University of Southampton, University Road, SO17 1BJ
Southampton, UK
ip1g08@soton.ac.uk

The sound transmission loss (STL) of a panel is often estimated using an infinite plate model. However, some discrepancies are found between these predicted results and experimental ones. One of the sources of such discrepancies corresponds to the finite extent that is naturally found in real structures. In the present study an analytical waveguide model of sound transmission is used to study the effect of finite dimensions in one direction for a panel which is long in the other dimension. The resulting model is used to investigate the effect of the finite width on the STL through a simple case of an infinite plate strip with simply supported boundary conditions. The results obtained are compared with those for the infinite plate. The resulting analytical model can also be used to validate numerical methods such as waveguide FE/BE.

1 Introduction

Most prediction models for calculating the sound transmission loss (STL) of panels were developed with the assumption that the panels are infinite in extent. Some of them used in practice include the prediction models of Beranek & Work [1], Cremer [2] and Sharp [3]. As real panels are always bounded, it is instructive to investigate the effect of the assumption on the predicted STL. Here, an analytical model is developed for an infinite plate strip in which the structure is assumed to be infinite in length but have a finite width, confined by parallel boundaries. Such structures can also be considered as waveguides [4].

Considering the structure to be finite in the *y*-direction a modal solution can be utilized to describe the structural response in terms of *y*. Meanwhile, for the *x*-direction, as the structure is infinite, a travelling wave solution is suitable to describe the dependence of displacement on *x*. By combining these solutions, the response of the plate strip is obtained in the wavenumber domain using the Fourier transform method.

The framework for deriving the exact solutions is readily available in e.g. [2, 4]. In those references, the structural vibration response and its interaction with surrounding fluid are discussed from a wave point of view. This wave approach has been applied to obtain solutions by utilizing a spatial Fourier transform for solving many basic cases e.g. beams, plates, pipes (or cylindrical structures), etc. Some results have also been found for the case of a plate strip.

The effect of the finite extent is discussed first by comparing the STL results of the plate strip and the infinite plate for normal and oblique incidence. The STL comparison under diffuse sound field excitation is also considered to give further insight into consequences of the finite extent in structures.

The resulting solutions can also be used as a benchmark solution for such waveguide structures, for example in validating waveguide finite element/boundary element approaches. In the present paper, example comparisons of the analytical and numerical results are provided.

2 Problem statement

In this section the sound transmission due to a plane acoustic wave acting on a simply supported plate strip (waveguide) is considered. The plate strip has width l_y in the *y*-direction and is infinite length in the *x*-direction. The incident plane wave impinges on the plate strip with elevation angle θ and azimuth angle φ as shown in Figure 2.1. Some simplifying assumptions should be noted as follows:

1. The plate strip is modelled with the thin-plate theory and it is set in an infinite rigid baffle.
2. The thickness of the baffle and the plate is neglected.
3. Simply supported boundaries are assumed.
4. The acoustic medium on both sides of the plate is assumed to be identical.
5. The amplitude of the reflected sound pressure is initially assumed equal to the incident sound pressure so that the blocked pressure field at the plate surface is equal to twice the incident pressure.

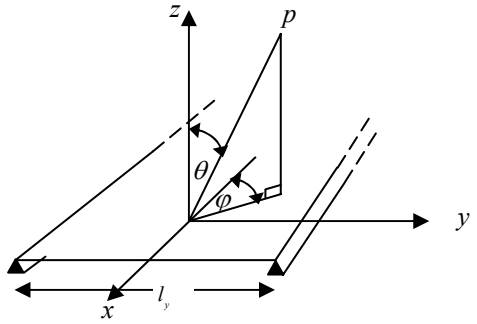

Figure 2.1. Direction of a plane wave incident on an infinite plate strip.

2.1 Pressure and velocity functions

The incident sound pressure is considered as a plane wave expressed by

$$p_i(x,y,z) = p_i e^{-ik_x x} e^{-ik_y y} e^{-ik_z z} \tag{1}$$

where a time harmonic dependence $e^{i\omega t}$ is assumed. The wavenumbers in *x*, *y* and *z* directions can be defined as:

$$k_z = k\cos\theta;\ k_x = \bar{k}\cos\varphi;\ k_y = \bar{k}\sin\varphi \tag{2}$$

where $\bar{k} = k\sin\theta$ and $k = \sqrt{k_x^2 + k_y^2 + k_z^2}$ is given by $k = \omega/c$ with ω the angular frequency and c the sound velocity.

The total pressure on the plate surface at $z = 0$ consists of the superposition of the blocked pressure field p_{bl} and the radiated pressure field p_{rad} on both sides of the plate. The radiated pressure terms will impose a fluid loading at the plate surface. The two-dimensional bending wave equation subject to the applied acoustic pressure field is

$$D'\left(\left(\frac{\partial^4 v}{\partial x^4} + 2\frac{\partial^4 v}{\partial x^2 \partial y^2} + \frac{\partial^4 v}{\partial y^4}\right) - k_B^4 v\right) = i\omega\left(p_{bl} + p_{rad}^- - p_{rad}^+\right) \tag{3}$$

The distribution of the pressure $p(x,y)$ may be expressed by the combination of a Fourier integral and a Fourier series. This yields

$$p(x,y)=\frac{1}{2\pi}\int_{-\infty}^{\infty}\sum_{m=1}^{\infty}p_m(\kappa)e^{-i\kappa x}\sin\left(m\pi y/l_y\right)d\kappa \quad (4)$$

and

$$p_m(\kappa)=\frac{2}{l_y}\int_0^{l_y}\int_{-\infty}^{\infty}p(x,y)e^{i\kappa x}\sin\left(m\pi y/l_y\right)dxdy \quad (5)$$

where m is an integer corresponding to each mode in the $y-$direction and κ is the (real) wavenumber in the $x-$direction.

It may be noted that

$$\int_{-\infty}^{\infty}e^{i(\kappa-k_x)x}dx=2\pi\delta(\kappa-k_x) \quad (6)$$

This gives

$$p(x,y)=\sum_{m=1}^{\infty}A_m\sin\left(m\pi y/l_y\right)e^{-ik_x x} \quad (7)$$

where

$$A_m=\frac{2}{l_y}\int_0^{l_y}\left(2p_i e^{-ik_y y'}+p^-_{rad}(y')-p^+_{rad}(y')\right)\sin\left(m\pi y'/l_y\right)dy' \quad (8)$$

Similarly, because the plate strip is uniform and infinite in the $x-$direction, its transverse velocity may be written conveniently in the form

$$v(x,y)=\sum_{m'=1}^{\infty}v_{y,m'}(y)e^{-ik_x x} \quad (9)$$

where m' is an integer designating each mode of the plate vibration and $v_{y,m'}(y)=v_{m'}\sin\left(m'\pi y/l_y\right)$. This transverse velocity is only defined for $0\le y\le l_y$ and is zero otherwise. Subsequently, it can be expressed in terms of an infinite set of simple harmonic waves travelling in the $y-$direction, with wavenumber denoted as γ in order to distinguish it from the incident wavenumber k_y, as follows

$$\tilde{V}_{y,m'}(\gamma)=\int_0^{l_y}v_{y,m'}(y)e^{i\gamma y}dy \quad (10)$$

$$v_{y,m'}(y)=\frac{1}{2\pi}\int_{-\infty}^{\infty}\tilde{V}_{y,m'}(\gamma)e^{-i\gamma y}d\gamma \quad (11)$$

The solution for $\tilde{V}_{y,m'}(\gamma)$ is

$$\tilde{V}_{y,m'}(\gamma)=v_{m'}a_{m'}(\gamma) \quad (12)$$

where

$$a_{m'}(\gamma)=\frac{(m'\pi/l_y)[(-1)^{m'}e^{i\gamma l_y}-1]}{[\gamma^2-\left(m'\pi/l_y\right)^2]} \quad (13)$$

In order to solve the coupled vibration-radiation problem, some boundary conditions must be satisfied, i.e. the fluid particle velocity must be equal to the normal plate velocity and the fluid particle velocity v and the pressure p must satisfy Euler's equation $i\omega\rho_0\vec{v}=-\vec{\nabla}p$. Hence the radiated pressure field, assuming the fluid on both sides is the same, is

$$p_{rad}(x,y)=\frac{1}{2\pi}\int_{-\infty}^{\infty}\sum_{m'=1}^{\infty}v_{m'}a_{m'}(\gamma)e^{-i\gamma y}e^{-i\kappa x}\left(\frac{\omega\rho_0}{k_z}\right)d\gamma \quad (14)$$

where $k_z=\sqrt{k^2-\kappa^2-\gamma^2}$. Note that $p^-_{rad}=-p^+_{rad}$.

Therefore, A_m in Eq.(8) becomes

$$A_m=\frac{2}{l_y}\left(2p_i a_m(k_y)-\frac{1}{\pi}\left(\int_{-\infty}^{\infty}\sum_{m'=1}^{\infty}v_{m'}a_{m'}(\gamma)a^*_m(\gamma)\left(\omega\rho_0/k_z\right)d\gamma\right)\right) \quad (15)$$

where $a_m(-\gamma)=a^*_m(\gamma)$, as the modal displacement function is real.

Substituting Eq. (7) and Eq. (9) into Eq. (3), this gives

$$\sum_{m'=1}^{\infty}\left(-\frac{iD'}{\omega}\left(\left(k_x{}^2+\left(m'\pi/l_y\right)^2\right)^2-k_B{}^4\right)\right)v_{m'}e^{-ik_x x}\times\sin\left(m'\pi y/l_y\right)=\sum_{m=1}^{\infty}A_m e^{-ik_x x}\sin\left(m\pi y/l_y\right) \quad (16)$$

Using the orthogonality of the mode shapes, Eq. (16) can be written for a single term in the series; to obtain this, it is multiplied with $\sin\left(m\pi y/l_y\right)$ and integrated over the width l_y yielding

$$\left[-\frac{iD'}{\omega}\left(\left(k_x{}^2+\left(m\pi/l_y\right)^2\right)^2-k_B{}^4\right)\right]v_m=A_m \quad (17)$$

and substituting A_m from Eq. (15) into Eq. (17) after some simplifications, it is found that

$$v_m=\left(4p_i a_m(k_y)/l_y\right)\times\frac{1}{\left[\left[-\frac{iD'}{\omega}\left(\left(k_x{}^2+\left(m\pi/l_y\right)^2\right)^2-k_B{}^4\right)\right]+\frac{2}{l_y\pi}\left(\int_{-\infty}^{\infty}\sum_{m'}a_{m'}(\gamma)a^*_m(\gamma)\left(\omega\rho_0/k_z\right)d\gamma\right)\right]} \quad (18)$$

where $k_z=\sqrt{k^2-\kappa^2-\gamma^2}$.

2.2 Sound transmission loss

The radiated sound power of the plate strip per unit length in the $x-$ direction $W_{rad\,2}$ is given by

$$W_{rad\,2} = \frac{1}{2}\mathrm{Re}\left\{\frac{1}{L_x}\int_{-\infty}^{\infty}\int_{0}^{L_x} p(x,y)v^*(x,y)dxdy\right\} \quad (19)$$

in which the range of the integration over y has been extended to $\pm\infty$ because the form of $\tilde{V}_y(\gamma)$ ensures that v_y is zero outside $0 < y < l_y$. Substituting Eq. (11) and Eq. (14) into Eq. (19) with the necessary condition $k_x^2 + \gamma^2 \le k^2$, this yields

$$W_{rad\,2} = \frac{1}{4\pi}\sum_{m=1}^{\infty}\sum_{m'=1}^{\infty}\left\{\int_{-\sqrt{k^2-k_x^2}}^{\sqrt{k^2-k_x^2}} \frac{\rho_0 ck}{\sqrt{k^2-k_x^2-\gamma^2}} \times \tilde{V}_{y,m}(\gamma)\tilde{V}^*_{y,m'}(\gamma)d\gamma\right\} \quad (20)$$

The incident power per unit length for the plate strip can be expressed as

$$W_{inc} = |p_i|^2 \cos(\theta) l_y / 2\rho_0 c \quad (21)$$

The transmission coefficient τ is given by ratio of the radiated power to the incident power, which gives

$$\tau = \frac{(\rho_0 c)^2}{2\pi |p_i|^2 \cos\theta}\left\{\sum_{m=1}^{\infty}\sum_{m'=1}^{\infty}\left\{\int_{-\sqrt{k^2-k_x^2}}^{\sqrt{k^2-k_x^2}} \frac{\rho_0 ck}{\sqrt{k^2-k_x^2-\gamma^2}} \times \tilde{V}_{y,m}(\gamma)\tilde{V}^*_{y,m'}(\gamma)d\gamma\right\}\right\} \quad (22)$$

The sound transmission loss R is found from

$$R = -10\log_{10}\tau \quad \text{dB} \quad (23)$$

3 Results

In this section, the STL results of a 1 m wide plate strip are compared with those of the infinite plate which are calculated using formulae from [4] and [2] for normal and oblique incidence. The plate strip is made of 6 mm aluminium with a loss factor of 0.1 assumed. The wavenumbers of free waves are shown inFigure 3.1. From this it can be seen that the first waves (with half a wavelength across the width) cut on at 14.8 Hz. Subsequent wave modes, with m half wavelengths across the width, cut on at m^2 times this first cut-on frequency.

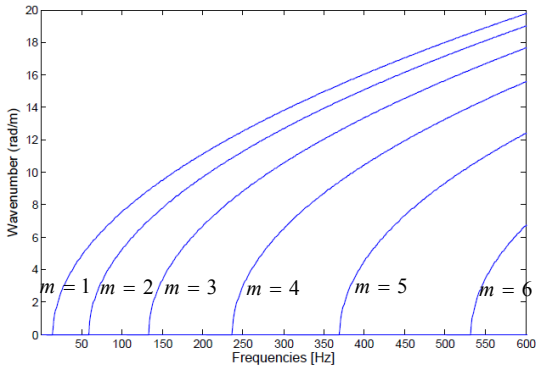

Figure 3.1 The dispersion curves of a simply-supported plate strip

3.1 Normal incidence

Figure 3.2 presents a comparison of the predicted STL between the plate strip and infinite plate. In general, at frequencies above 100 Hz, the STL of the plate strip tends to the infinite plate result which typically follows the mass-law behaviour. Hence, for this region the STL of the plate strip is mass-controlled. Some dips or ripples are found in the curves that are related to cut-on frequencies of different waves in the plate while such features are not present in the infinite plate model. At low frequency, or $\omega << \omega_1$, a stiffness-controlled behaviour appears where a slope of -30 dB/decade occurs rather than -20 dB/decade found for the infinite plate model. At the first cut-on frequency ω_1, the transmission loss has a negative value rather than zero as the lowest value which appears in the infinite plate model. This happens as the incident sound is normalized to the area of the plate whereas power can also be transmitted from a wider area by diffraction. Hence the ratio of radiated sound power and incident power can be greater than unity for the case of the plate strip which has a finite dimension in one direction. A more detailed discussion on this issue is given in [5].

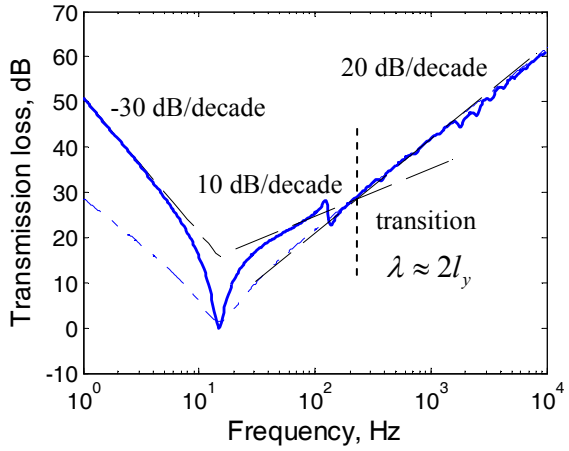

Figure 3.2. STL comparison of the plate strip and the infinite plate for normal incident case (— plate strip; --- STL slope of plate strip; – • – infinite plate).

The slope of the STL curve in Figure 3.2 changes from 10 dB/decade to 20 dB/decade at about 200 Hz. This frequency corresponds to $\lambda \approx 2l_y$. Thus, below this

frequency the plate strip is narrow compared with the wavelength and it radiates as a line source whereas above this frequency it radiates as an area. This also affects the slope at low frequency as noted above.

3.2 Oblique incidence

Figure 3.3 shows results for different angles of incidence about the x axis with $\varphi = 90^{\circ}$. The coincidence frequency depends on the incident angle, with a higher angle corresponding to a lower coincidence frequency. These results have a similar tendency to those obtained by the infinite plate model which is calculated following [2].

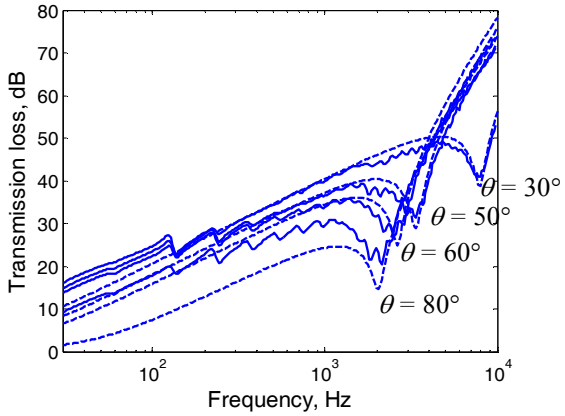

Figure 3.3. STL of the plate strip and the infinite plate for oblique incidence (— plate strip; --- infinite plate).

However, in the area close to the coincidence frequency the STL of the infinite plate tends to be higher than that of the plate strip. This difference is affected by the presence of edge mode radiation and cut-on frequencies in the plate strip response. Conversely, when the incident angle is getting larger, it can be seen that the STL of the infinite plate is lower than that obtained by the plate strip model for frequencies below the coincidence frequency. This is caused by the influence of the radiation ratio of the infinite plate which increases as the incident angle increases and becomes infinite when $\theta = 90^{\circ}$ while that of a finite structure remains finite [6].

3.3 Diffuse sound field

The diffuse sound field excitation is formulated as the superposition of uncorrelated plane waves with equal amplitude in all direction. The sound transmission is then obtained by integrating the response of all incident plane waves over the incident angle and weighting them with the solid angle to account for the directional distribution. The diffuse sound transmission loss is calculated using 9 incident angles about the x axis and 18 incidence angles about the y axis. An upper elevation angle $\theta_{\text{lim}} = 90^{\circ}$ corresponds to the full random incidence case [7].

Figure 3.4 presents a comparison of the sound transmission loss between the plate strip and the infinite plate for the diffuse field case. It is clear that the dip at around 2 kHz is associated with the critical frequency. Above this frequency, the plate strip and the infinite plate produce a similar curve. However, below this frequency the STL of the plate strip is higher by 6.5 dB at low frequency than that of the infinite plate. This difference reduces with increasing frequency. It comes about because a finite extent in one dimension of the plate strip introduces a spatial windowing effect on the infinite baffle [6]. Accordingly, the radiation ratio of the infinite plate is modified to remain finite for increasing incident angle rather than becoming infinite. This leads to a higher STL for the plate strip. This situation is also illustrated in Figure 3.3 for oblique incidence.

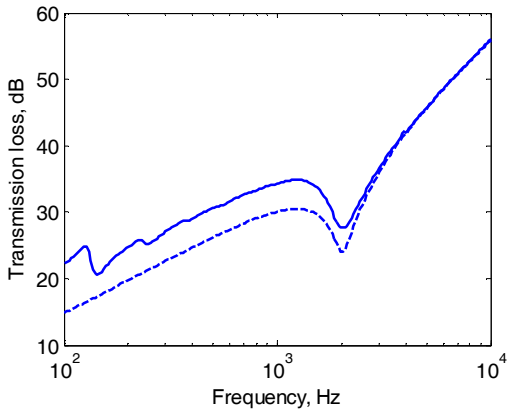

Figure 3.4. STL of plate strip under a diffuse sound field excitation (— Plate strip; --- infinite plate).

4 Comparison of analytical and numerical model results

To demonstrate the capability of the analytical model to be used as a benchmark solution, the analytical model results are compared with those obtained by a numerical model. The numerical model is developed based on the coupled Waveguide Finite Element-Wavedomain Boundary Element (WFBE) method [8] and is realized using eight-noded quadrilateral solid elements with quadratic polynomial shape functions. Meanwhile, a three-noded quadrilateral element is used for the WBE fluid. The BE mesh is extended by 1 m on both sides beyond the width of the plate strip to represent the rigid baffle.

4.1 Normal and oblique incidence

Figure 4.1(a) presents a comparison of the STL for the analytical model and the numerical one and for the normal incidence case. At frequencies above 50 Hz, the results of the analytical model agree well with those of the numerical one. Below this frequency, the discrepancy is due to the finite baffle width; hence it will always appear depending on the assumed baffle length considered in the numerical model.

For the case of oblique incidence about the x axis, the results are shown in Figure 4.1(b). The analytical model generally produces similar results to the numerical ones below the coincidence frequency. A similar situation is also evident for the case of oblique incidence about the y axis as shown in Figure 4.1(c). This is indicated by the overall STL behaviour below and at the coincidence frequency.

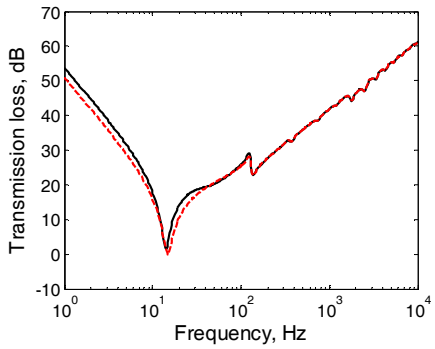

(a)

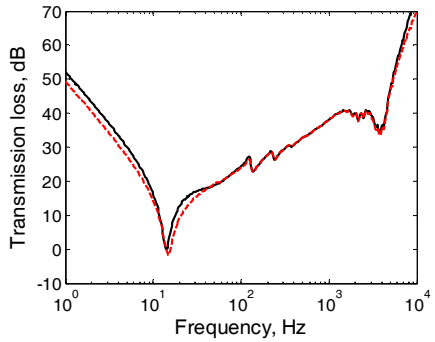

(b)

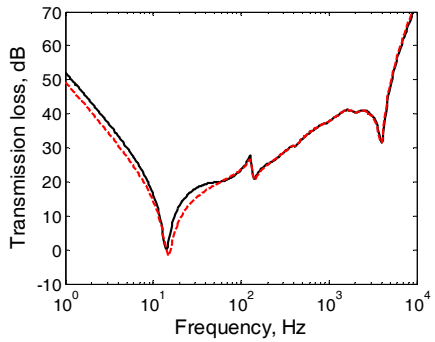

(c)

Figure 4.1. STL for normal and oblique incidence: (a) normal incidence; (b) at 45º about x axis; (c) at 45º about y axis (— numerical model --- analytical model).

4.2 Diffuse sound field excitation

The diffuse sound field is represented by the full random incidence (or $\theta_{\text{lim}} = 90^{\circ}$). These results are shown in Figure 4.2. From this, the analytical model produces a good result compared with that of the numerical model.

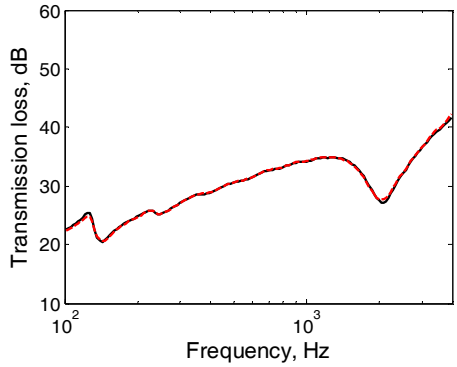

Figure 4.2. STL of the numerical model and the analytical model under a diffuse sound field excitation (— numerical model; --- analytical model)

5 Conclusion

The sound transmission loss of the plate strip for normal incidence converges to the mass-law result at high frequencies. At low frequency, below the first cut-on frequency, a stiffness-controlled region appears, while the mass-controlled region exists above the first cut-on frequency. The slope at low frequencies is modified from the result for an infinite plate when the width is less than half the acoustic wavelength. Some dips or ripples in the curve are related to edge mode radiation and various cut-on frequencies. Such features are introduced by finite extent that are not present in an infinite model.

Acknowledgments

The first author is grateful to Directorate General of Higher Education (DGHE), Department of National Education of Indonesia for providing a postgraduate scholarship. The authors also would like to acknowledge help and assistance in using WANDS from Dr Jungsoo Ryue from School of Naval Architecture and Ocean Engineering, University of Ulsan, Korea.

References

[1] Beranek, L.L. and G.A. Work, Sound transmission through multiple structures containing flexible blankets. The Journal of the Acoustical Society of America, 1949. 21(4): p. 419-428.

[2] Cremer, L., M. Heckel, and B.A.T. Petterson, Structure-Borne Sound. 3rd edition ed. 2005, Berlin: Springer.

[3] Sharp, B.H., Prediction Methods for the Sound Transmission of Building Elements. Noise Control Engineering, 1978. 11(2): p. 53-63.

[4] Fahy, F. and P. Gardonio, Sound and Structural Vibration: Radiation, Transmission and Response. 2nd ed. 2006, London: Academic Press.

[5] Thompson, D.J., P. Gardonio, and J. Rohlfing, Can a transmission coefficient be greater than unity? Applied Acoustics, 2009. 70(5): p. 681-688.

[6] Villot, M., C. Guigou, and L. Gagliardini, Predicting the acoustical radiation of finite size multi-layered structures by applying spatial windowing of infinite structures. Journal of Sound and Vibration, 2001. 245(3): p. 433-455.

[7] Beranek, L.L., Noise and Vibration Control 1971, New York: McGraw-Hill

[8] Nilsson, C.-M. and C.J.C. Jones, Theory manual for WANDS 2.1, ISVR technical memorandum No.975. 2007, University of Southampton: UK.